Spontaneous torque on an inhomogeneous chiral body out of thermal equilibrium

Kimball A. Milton, 1,* Nima Pourtolami, 2,† and Gerard Kennedy, 3,‡

¹H. L. Dodge Department of Physics and Astronomy, University of Oklahoma, Norman, Oklahoma 73019, USA ²National Bank of Canada, Montreal, Quebec, Canada H3B 4S9

³School of Mathematical Sciences, University of Southampton, Southampton SO17 1BJ, England, United Kingdom



(Received 3 December 2024; accepted 3 February 2025; published 25 February 2025)

In a previous paper we showed that an inhomogeneous body in vacuum will experience a spontaneous force if it is not in thermal equilibrium with its environment. This is due to the asymmetric asymptotic radiation pattern such an object emits. We demonstrated this self-propulsive force by considering an expansion in powers of the electric susceptibility: A torque arises in first order, but only if the material constituting the body is nonreciprocal. No force arises in first order. A force does occur for bodies made of ordinary (reciprocal) materials in second order. Here we extend these considerations to the torque. As one would expect, a spontaneous torque will also appear on an inhomogeneous chiral object if it is out of thermal equilibrium with its environment. Once a chiral body starts to rotate, it will experience a small quantum frictional torque, but much more important, unless a mechanism is provided to maintain the nonequilibrium state, is thermalization: The body will rapidly reach thermal equilibrium with the vacuum, and the angular acceleration will essentially become zero. For a small, or even a large, inhomogeneous chiral body, a terminal angular velocity will result, which seems to be in the realm of observability.

DOI: 10.1103/PhysRevA.111.022815

I. INTRODUCTION

There is extensive theoretical literature over recent decades concerning quantum electrodynamic friction between two relatively moving surfaces, or between a particle or atom moving parallel to a conducting or dielectric surface; see Refs. [1–19], for example. But much earlier, Einstein and Hopf [20] showed that a polarizable particle moving with nonrelativistic velocity v through vacuum, filled with blackbody radiation at temperature $T = \beta^{-1}$, experiences a frictional force, which can be expressed in generalized form for an isotropic particle with polarizability $\alpha(\omega)$:

$$F^{\rm EH} = -\frac{v\beta}{12\pi^2} \int_0^\infty d\omega \, \omega^5 {\rm Im} \, \alpha(\omega) \frac{1}{\sinh^2 \beta \omega/2}. \tag{1.1}$$

Here, the imaginary part of the polarizability may arise from either intrinsic processes within the particle or, for the case of an atom, fluctuations in the electromagnetic field. In the last two decades there has been considerable work on this effect: For a subset of the literature see Refs. [21–26]. But such a force is very small, and has never been observed. We generalized this result to relativistic velocities in Refs. [27,28], where

*Contact author: kmilton@ou.edu

†Contact author: nima.pourtolami@gmail.com ‡Contact author: g.kennedy@soton.ac.uk

Published by the American Physical Society under the terms of the Creative Commons Attribution 4.0 International license. Further distribution of this work must maintain attribution to the author(s) and the published article's title, journal citation, and DOI.

the force might be much more appreciable. In particular, we considered the temperature of the particle, T', to be different from that of the background, T. We found that the nonequilibrium steady state (NESS) [29], where the particle neither gains nor loses energy in its rest frame, requires that the ratio of these two temperatures, T'/T, has a definite value, different from unity, which might prove to be a signature for quantum vacuum friction. The NESS condition plays a role analogous to thermal equilibrium in this dynamic context and reduces to thermal equilibrium when the relative velocity between the body and its environment vanishes, in which case $T'/T \rightarrow 1$.

Even more remarkably, a stationary body may experience a force or torque in a nontrivial background [30,31], or in vacuum [32-41], provided it is out of thermal equilibrium with its environment. In particular, for a nonreciprocal body [42], that is, one for which the electric susceptibility has a nonsymmetric real part, a spontaneous torque can arise in vacuum if the temperature of the body differs from that of the vacuum [39,40,43,44]. No force can arise, however, in first order in the susceptibility, unless another body, such as a conducting plate, is present. Such forces and torques owe their origin to radiative heat transfer [45].

Forces and torques on ordinary bodies made of reciprocal materials also arise, but in higher order in the electric susceptibility. Müller and Krüger [46] showed that a Janus ball with the two halves made of different homogeneous reciprocal materials would experience a force, for which they gave an expression in the dilute approximation, in second order in the susceptibility. Shortly thereafter, this effect was confirmed by Reid et al. [47] through numerical calculations, but those authors found a different scaling behavior with the radius of the ball. To achieve a spontaneous force, to second order in electric susceptibility, requires that the body not only be out of thermal equilibrium with its environment, but also that it be inhomogeneous, having an electric susceptibility that varies over the body. Of course, the distribution of susceptibility must break reflection invariance so there is an axis for motion. According to Ref. [47], however, the inhomogeneity requirement is not necessary for a torque to appear; all that is required is that the body be chiral, that is, have a "handedness."

In this paper we continue our systematic treatment of quantum-thermal vacuum torques and forces. In Ref. [48] we started from the classical expression for the force on a dielectric body, and expanded it out to fourth order in generalized susceptibilities (i.e., the electric susceptibility or the Green's dyadic) and quantized the result by using the fluctuation-dissipation theorem (FDT). In this way we obtained expressions for the force on an inhomogeneous object out of thermal equilibrium with its vacuum environment, which we evaluated for a number of examples. The results were in qualitative agreement with previous work [46,47,49]. Of course, the fact that the body was hotter or colder than its environment meant that it would rapidly thermalize, but even so, the resulting terminal velocity might be observable.

Here, we return to the torque, but consider it in second order in the electric susceptibility. To achieve a nonzero torque in second order, the body again must be out of thermal equilibrium with the vacuum, be chiral to break rotational and reflection invariance, and be inhomogeneous. This is in contrast to the nonperturbative numerical work of Ref. [47], which finds a torque for a chiral body made of isotropic and uniform gold.

The outline of this paper is as follows. In Sec. II we first rederive the torque on a nonreciprocal body, which occurs in first order in the electric susceptibility. We then expand the expression for the torque to second order and find that a torque arises in general for a reciprocal body provided it is chiral and inhomogeneous. In Sec. III we rederive the general torque expression we found in Sec. II by examining the radiation-zone electromagnetic fields through the angular momentum flux vector. We then consider two simple examples which would exhibit a torque but not a force (so the body might be observed for some time without it flying away). In Sec. IV we examine what we dub a dual Allen wrench, with dielectric tags perpendicularly attached to a central metal wire. The torque and resulting terminal angular velocity may be enhanced if the tags are replaced by two-dimensional flags, which we discuss in Sec. V. Conclusions round out the paper. Two Appendixes follow, one on the general expansion scheme in susceptibilities, Appendix A, and one on the duality between dielectric-metal and blackbody-metal composites, Appendix B.

We use natural units, $\hbar = c = \epsilon_0 = \mu_0 = k_B = 1$.

II. TORQUE: SOURCE POINT OF VIEW

Classically, the torque on a stationary dielectric body with polarization vector \mathbf{P} is given by [50]

$$\tau = \int (d\mathbf{r}) \frac{d\omega}{2\pi} \frac{d\nu}{2\pi} e^{-i(\omega+\nu)t} [\mathbf{P}(\mathbf{r};\omega) \times \mathbf{E}(\mathbf{r};\nu) + P_i(\mathbf{r};\omega)(\mathbf{r}\times\nabla) E_i(\mathbf{r};\nu)]. \tag{2.1}$$

The first term here is called the internal torque and the second the external torque, because the latter is reflective of the force on the body.

A. First-order calculation

Let us first review how this yields, in first order in the susceptibility, a torque if the body is out of thermal equilibrium with the vacuum. To do this we either expand E to first order in P,

$$E_i^{(1)}(\mathbf{r};\omega) = \int (d\mathbf{r}')\Gamma_{ij}(\mathbf{r} - \mathbf{r}';\omega)P_j(\mathbf{r}';\omega), \qquad (2.2a)$$

where Γ is the vacuum retarded Green's dyadic, or we expand **P** to first order in **E**,

$$P_i^{(1)}(\mathbf{r};\omega) = \chi_{ii}(\mathbf{r};\omega)E_i(\mathbf{r};\omega), \qquad (2.2b)$$

where we assume that the electric susceptibility χ is local in space. These expressions give the first-order linear responses to the fluctuating fields \mathbf{P} and \mathbf{E} , respectively. See Appendix A for the general scheme of the expansion. The resulting terms, due to expanding \mathbf{P} once, denoted (1,0), or expanding \mathbf{E} once, (0,1), are then quantized using the FDT for the independent fluctuating fields:

$$\langle P_{j}(\mathbf{r};\omega)P_{l}(\mathbf{r}';\nu)\rangle = 2\pi\delta(\omega+\nu)\delta(\mathbf{r}-\mathbf{r}')$$

$$\times\Im\chi_{jl}(\mathbf{r};\omega)\coth\frac{\beta'\omega}{2},$$
(2.3a)

$$\langle E_{j}(\mathbf{r};\omega)E_{l}(\mathbf{r}';\nu)\rangle = 2\pi\delta(\omega+\nu)\Im\Gamma_{jl}(\mathbf{r}-\mathbf{r}';\omega)\coth\frac{\beta\omega}{2},$$
(2.3b)

where $T = 1/\beta$ is the temperature of the blackbody environment, and $T' = 1/\beta'$ is the temperature of the body, and symmetrized products of fields are assumed.³ The FDT requires that the "imaginary part" appearing here be the anti-Hermitian part:

$$\Im \mathbf{\chi} \equiv \frac{1}{2i} (\mathbf{\chi} - \mathbf{\chi}^{\dagger}). \tag{2.4}$$

(The vacuum is, of course, reciprocal, which means $\Im \Gamma = \operatorname{Im} \Gamma$, the ordinary imaginary part.) In this order, the Green's

¹There appear to be different results in the literature for the dependence of the force on the size of the Janus ball. For example, the dependence we found in Ref. [48] for the second-order susceptibility contribution to the force disagrees with that given in Refs. [46,47], which do not seem to agree with each other.

²Here, (n, m) designates the number of iterations in the expansion of **P** and **E**, respectively.

³Note that, at zero temperature, the fluctuations are purely quantum, while, in the limit of infinite temperature, the fluctuations are purely classical. In between, the fluctuations are thermal but reflect the quantum nature of the system. This is easily seen on reinstating conventional units, and recognizing that the thermal factor $(e^{\hbar\omega/k_BT}-1)^{-1}$ explicitly involves both \hbar and k_B .

dyadics are evaluated at coincident points,

$$\Gamma(\mathbf{r} - \mathbf{r}'; \omega) \to \mathbf{1} \left(\frac{\omega^2}{6\pi R} + i \frac{\omega^3}{6\pi} + O(R) \right), \ R = |\mathbf{r} - \mathbf{r}'| \to 0,$$
 (2.5)

and its gradient is odd in $\mathbf{r} - \mathbf{r}'$. This means that the external torque vanishes, which is the reason there can be no spontaneous force in this order. From the internal torque, we immediately obtain the sum of the (1,0) and (0,1) contributions:

$$\tau_{i} = \int (d\mathbf{r}) \frac{d\omega}{2\pi} \epsilon_{ijk} \operatorname{Re} \chi_{jk}(\mathbf{r}; \omega) \frac{\omega^{3}}{6\pi} \left(\coth \frac{\beta \omega}{2} - \coth \frac{\beta' \omega}{2} \right). \tag{2.6}$$

Therefore, a spontaneous vacuum torque can arise only for a nonreciprocal material, which possesses a nonsymmetric real part of the electric susceptibility.⁴ This is exactly the result found in Refs. [39,40,43,44].

B. Second-order torque

To obtain a torque on a body made of reciprocal material, we have to go to second order in the electric susceptibility. To deal with the greater complexity, let us start with the terms coming from PP fluctuations. Using the designation above, these involve two contributions, (2,1) and (0,3). The former is

$$\tau_{i}^{(2,1)} = \int (d\mathbf{r})(d\mathbf{r}')(d\mathbf{r}'') \frac{d\omega}{2\pi} \frac{d\nu}{d\pi} \epsilon_{ijk} \Big[\chi_{jm}(\mathbf{r};\omega) \Gamma_{mn}(\mathbf{r} - \mathbf{r}';\omega) P_{n}(\mathbf{r}';\omega) \Gamma_{kl}(\mathbf{r} - \mathbf{r}'';\nu) P_{l}(\mathbf{r}'';\nu) + \chi_{lm}(\mathbf{r};\omega) \Gamma_{mn}(\mathbf{r} - \mathbf{r}';\omega) P_{n}(\mathbf{r}';\omega) \Gamma_{lp}(\mathbf{r} - \mathbf{r}'';\nu) P_{p}(\mathbf{r}'';\nu) \Big].$$
(2.7)

Use of the FDT (2.3a) yields

$$\tau_{i}^{(2,1)} = \int (d\mathbf{r})(d\mathbf{r}') \frac{d\omega}{2\pi} \epsilon_{ijk} \Big[\chi_{jm}(\mathbf{r};\omega) \Gamma_{mn}(\mathbf{r} - \mathbf{r}';\omega) \Im \chi_{nl}(\mathbf{r}';\omega) \Gamma_{kl}(\mathbf{r} - \mathbf{r}';-\omega) + \chi_{lm}(\mathbf{r};\omega) \Gamma_{mn}(\mathbf{r} - \mathbf{r}';\omega) \Im \chi_{np}(\mathbf{r}';\omega) r_{j} \nabla_{k} \Gamma_{lp}(\mathbf{r} - \mathbf{r}';-\omega) \Big] \coth \frac{\beta'\omega}{2}.$$
(2.8)

A small check of this is that if in the second term, the external part, we substitute $\mathbf{r} \to \mathbf{r} + \mathbf{R}$, where \mathbf{R} designates the position of the center of mass of the body, we read off the force contribution found in Ref. [48]:

$$F_k^{(2,1)} = \int (d\mathbf{r})(d\mathbf{r}') \frac{d\omega}{2\pi} \chi_{lm}(\mathbf{r};\mu) \Gamma_{mn}(\mathbf{r} - \mathbf{r}';\omega) \Im \chi_{np}(\mathbf{r}';\omega) \nabla_k \Gamma_{lp}(\mathbf{r} - \mathbf{r}';-\omega) \coth \frac{\beta'\omega}{2}. \tag{2.9}$$

The formula for the torque simplifies considerably if the susceptibility is both isotropic and homogeneous, $\chi_{lm}(\mathbf{r};\omega) = \delta_{lm}\chi(\omega)$. Then,

$$\tau_{i}^{(2,1)} = \int (d\mathbf{r})(d\mathbf{r}') \frac{d\omega}{2\pi} \epsilon_{ijk} \operatorname{Im}[\chi(\omega)] \chi(\omega) [\Gamma_{jl}(\mathbf{r} - \mathbf{r}'; \omega) \Gamma_{kl}(\mathbf{r} - \mathbf{r}'; -\omega) + \Gamma_{ml}(\mathbf{r} - \mathbf{r}'; \omega) r_{j} \nabla_{k} \Gamma_{ml}(\mathbf{r} - \mathbf{r}'; -\omega)] \coth \frac{\beta'\omega}{2}.$$
(2.10)

This evidently vanishes: the second term, the external contribution, is zero, because it is odd under interchange of \mathbf{r} and \mathbf{r}' [$r_j \to \frac{1}{2}(r_j + r_j')$ to survive the Levi-Civita symbol], and the first term (the internal term) is zero because the vacuum Green's dyadic is entirely constructed from the vector $\mathbf{r} - \mathbf{r}'$. If the body is homogeneous but not isotropic, $\chi(\mathbf{r}; \omega) = \chi(\omega)$, it is similarly seen that the torque around any principal axis is zero.

If we assume isotropy only, but not homogeneity, it is still true that the internal torque vanishes, and we are left with

$$\tau_i^{(2,1)} = \int (d\mathbf{r})(d\mathbf{r}') \frac{d\omega}{2\pi} \epsilon_{ijk} \text{Im}[\chi(\mathbf{r}';\omega)] \chi(\mathbf{r};\omega) \Gamma_{ml}(\mathbf{r} - \mathbf{r}';\omega) r_j \nabla_k \Gamma_{ml}(\mathbf{r} - \mathbf{r}';-\omega) \coth \frac{\beta'\omega}{2}. \tag{2.11}$$

In the same way, we can write down the (0,3) contribution:

$$\tau_{i}^{(0,3)} = \int (d\mathbf{r})(d\mathbf{r}') \frac{d\omega}{2\pi} \epsilon_{ijk} \Big[\Im \chi_{jm}(\mathbf{r};\omega) \Gamma_{kl}(\mathbf{r} - \mathbf{r}'; -\omega) \chi_{ln}(\mathbf{r}'; -\omega) \Gamma_{nm}(\mathbf{r} - \mathbf{r}'; -\omega) + \Im \chi_{lp}(\mathbf{r};\omega) r_{j} \nabla_{k} [\Gamma_{lm}(\mathbf{r} - \mathbf{r}'; -\omega)] \chi_{mn}(\mathbf{r}'; -\omega) \Gamma_{np}(\mathbf{r} - \mathbf{r}'; -\omega) \Big] \coth \frac{\beta'\omega}{2}.$$
(2.12)

⁴Since the typical way such a nonreciprocity can arise is through an external magnetic field, calling this a vacuum effect seems to be an oxymoron.

⁵This notation means expanding the torque to a term quadratic in $\bf P$ and then using the FDT (2.3a). The EE notation means expanding to a term quadratic in $\bf E$ and then using the FDT (2.3b).

The second, external term, indeed reproduces the (0,3) force contribution found in Ref. [48]. And again it is readily seen that if the body is isotropic, so that $\chi_{ij}(\mathbf{r};\omega) = \delta_{ij}\chi(\mathbf{r};\omega)$, the internal torque vanishes, while if the susceptibility is homogeneous, the entire torque vanishes. However, if the susceptibility is isotropic but inhomogeneous, the external torque is nonzero—as it must be since there is a force in such a case—resulting in the torque due to PP fluctuations:

$$\tau_{i}^{(0,3)+(2,1)} = \tau_{i}^{PP} = -\int (d\mathbf{r})(d\mathbf{r}') \frac{d\omega}{2\pi} \epsilon_{ijk} r_{j}$$

$$\times \operatorname{Im}\Gamma_{lm}(\mathbf{r} - \mathbf{r}'; \omega) \nabla_{k} \operatorname{Im}\Gamma_{lm}(\mathbf{r} - \mathbf{r}'; \omega)$$

$$\times X(\mathbf{r}, \mathbf{r}'; \omega) \coth \frac{\beta'\omega}{2}, \qquad (2.13)$$

where

$$X(\mathbf{r}, \mathbf{r}'; \omega) = \operatorname{Im} \chi(\mathbf{r}; \omega) \operatorname{Re} \chi(\mathbf{r}'; \omega) - \operatorname{Re} \chi(\mathbf{r}; \omega) \operatorname{Im} \chi(\mathbf{r}'; \omega).$$
(2.14)

The second-order EE fluctuation contribution to the torque is calculated in the same way, and results merely in the change of sign and the replacement of the thermal factor $\coth \frac{\beta'\omega}{2}$ by $\coth \frac{\beta\omega}{2}$. For a body with isotropic susceptibility there is only the external torque, which is

$$\tau_{i} = \int \frac{d\omega}{2\pi} \left(\coth \frac{\beta \omega}{2} - \coth \frac{\beta' \omega}{2} \right) \epsilon_{ijk} \int (d\mathbf{r})(d\mathbf{r}')$$

$$\times X(\mathbf{r}, \mathbf{r}'; \omega) \operatorname{Im} \Gamma_{lm}(\mathbf{r} - \mathbf{r}'; \omega) r_{j}$$

$$\times \nabla_{k} \operatorname{Im} \Gamma_{lm}(\mathbf{r} - \mathbf{r}'; \omega), \qquad (2.15)$$

which yields the corresponding force found in Ref. [48]. Again, there is no torque or force unless the body is inhomogeneous. This is in contrast to the conclusions of the numerical work by Reid *et al.* [47], who find a torque on a homogeneous gold body that breaks chiral symmetry, such as a pinwheel; however, their method is nonperturbative. The product of Green's dyadics sandwiching the gradient operator can be written as

$$\frac{1}{2}\nabla \frac{2\Delta(\omega s)}{(4\pi s^3)^2} = \frac{1}{(4\pi)^2} \frac{\hat{\mathbf{s}}}{s^7} \phi(v), \tag{2.16}$$

with $\mathbf{s} = \mathbf{r} - \mathbf{r}'$ and $s = |\mathbf{s}|$, where, according to Ref. [48],

$$\Delta(v) = (3 - 2v^2 + v^4)\sin^2 v - v(3 - v^2)\sin 2v + 3v^2\cos^2 v,$$
(2.17)

in terms of $v = \omega s$. The result of differentiation gives [this is what we called $v^7D(v)$ in Ref. [48]]

$$\phi(v) = -9 - 2v^2 - v^4 + (9 - 16v^2 + 3v^4)\cos 2v + v(18 - 8v^2 + v^4)\sin 2v.$$
 (2.18)

Thus, Eq. (2.15) can be written as

$$\tau = -\int \frac{d\omega}{2\pi} \left(\coth \frac{\beta \omega}{2} - \coth \frac{\beta' \omega}{2} \right) \times \int (d\mathbf{r})(d\mathbf{r}') X(\mathbf{r}, \mathbf{r}'; \omega) \frac{\mathbf{r} \times \mathbf{r}'}{(4\pi)^2 s^8} \phi(v).$$
(2.19)

The examples we consider in Ref. [48] consisted of heterogeneous bodies consisting of two homogeneous parts, A and

B. The antisymmetric susceptibility product X becomes

$$\frac{1}{2}X(\mathbf{r}, \mathbf{r}'; \omega) \to X_{AB}(\omega)$$

$$= \operatorname{Im} \chi_A(\omega) \operatorname{Re} \chi_B(\omega) - \operatorname{Re} \chi_A(\omega) \operatorname{Im} \chi_B(\omega), \qquad (2.20)$$

where the spatial support of χ_A is the volume A, while the spatial support of χ_B is the nonoverlapping volume B. The torque in this situation can then be written as

$$\boldsymbol{\tau} = \frac{1}{2\pi^2} \int_0^\infty \frac{d\omega}{2\pi} X_{AB}(\omega) \left(\frac{1}{e^{\beta\omega} - 1} - \frac{1}{e^{\beta'\omega} - 1} \right) \mathbf{J}_{AB}(\omega), \tag{2.21a}$$

where the geometric factor is

$$\mathbf{J}_{AB}(\omega) = -\int_{A} (d\mathbf{r}) \int_{B} (d\mathbf{r}') \frac{\mathbf{r} \times \mathbf{r}'}{|\mathbf{r} - \mathbf{r}'|^{8}} \phi(\omega |\mathbf{r} - \mathbf{r}'|). \quad (2.21b)$$

That the integral is convergent is evident from the behavior of ϕ for small argument:

$$\phi(v) \sim -\frac{4}{9}v^8 + \frac{28}{225}v^{10} + \dots, \quad v \ll 1,$$
 (2.22a)

$$\phi(v) \sim -v^4 + v^5 \sin 2v + 3v^4 \cos 2v + \cdots, \quad v \gg 1.$$
 (2.22b)

It is worth noting that $\phi(v) + 4v^8/9$ is strictly positive.

III. TORQUES FROM RADIATION-ZONE FIELDS

Because of the discrepancy with the results of Ref. [47], it would be well to compute the torque in a different manner. Such is provided by the local conservation law of angular momentum [50]:

$$\partial_t \mathcal{J} + \nabla \cdot \mathcal{K} + \mathbf{r} \times \mathbf{f} = 0. \tag{3.1}$$

Here, the torque density is $\mathbf{r} \times \mathbf{f}$, in terms of the force density \mathbf{f} ; \mathscr{J} is the angular momentum density of the field, in vacuum,

$$\mathcal{J} = \mathbf{r} \times \mathbf{G}, \quad \mathbf{G} = \mathbf{E} \times \mathbf{H}; \tag{3.2a}$$

and \mathcal{K} is the angular momentum flux tensor,

$$\mathcal{K} = -\mathbf{T} \times \mathbf{r}, \quad \mathbf{T} = \frac{E^2 + H^2}{2} \mathbf{1} - \mathbf{E}\mathbf{E} - \mathbf{H}\mathbf{H}, \quad (3.2b)$$

in terms of the vacuum field momentum G and the electromagnetic stress tensor T. For our static situation, we may ignore the time derivative term in Eq. (3.1) (it will vanish when the FDT is applied). Now integrate this over a very large ball with origin at the center of the body. If the radius R of the sphere is very large compared to distance within the body, we have

$$\tau = \oint d\Omega R^2 \,\hat{\mathbf{R}} \cdot \mathbf{T} \times \mathbf{R} = -\oint d\Omega R^2 \,\hat{\mathbf{R}} \cdot (\mathbf{E}\mathbf{E} + \mathbf{H}\mathbf{H}) \times \mathbf{R}.$$
(3.3)

A. First-order torque

Let us first rederive the first-order torque for a nonreciprocal body. In that case it is clear that the **EE** contribution to the stress tensor is the only term that survives in the radiation zone. (The **HH** contribution brings in extra derivatives.) We expand the torque as before, but now we have to go to second order in generalized susceptibilities: (0,2) and (2,0)

correspond to EE fluctuations, while (1,1) corresponds to PP fluctuations.⁶ Let us concentrate on the latter:

$$\tau_i^{\text{PP}} = -\int (d\mathbf{r})(d\mathbf{r}') \frac{d\omega}{2\pi} \frac{d\nu}{2\pi} \hat{R}_l \Gamma_{lm}(\mathbf{R} - \mathbf{r}; \omega) P_m(\mathbf{r}; \omega) \epsilon_{ijk}$$
$$\times \Gamma_{jn}(\mathbf{R} - \mathbf{r}'; \nu) P_n(\mathbf{r}'; \nu) R_k e^{-i(\omega + \nu)t}. \tag{3.4}$$

If we apply the FDT, this turns into

$$\tau_{i}^{\text{PP}} = -\int (d\mathbf{r}) \frac{d\omega}{2\pi} \hat{R}_{l} \Gamma_{lm}(\mathbf{R} - \mathbf{r}; \omega) \Im \chi_{mn}(\mathbf{r}; \omega) \epsilon_{ijk}$$
$$\times \Gamma_{jn}(\mathbf{R} - \mathbf{r}; -\omega) R_{k} \coth \frac{\beta'\omega}{2}. \tag{3.5}$$

We need to keep the two leading terms in the Green's dyadic here (in this case we can drop \mathbf{r} in comparison to \mathbf{R}):

$$\mathbf{\Gamma}(\mathbf{R};\omega) \sim \frac{e^{i\omega R}}{4\pi} \left[\frac{\omega^2}{R} (\mathbf{1} - \mathbf{\hat{R}\hat{R}}) + \frac{i\omega}{R^2} (\mathbf{1} - 3\mathbf{\hat{R}\hat{R}}) \right], \quad R \gg r, \ r'.$$
(3.6)

The reason the higher-order term must be included here is that the \hat{R}_l annihilates the leading term in the first Green's dyadic. Integrating over the large sphere gives

$$\oint d\Omega R_l R_m = \frac{4\pi}{3} \delta_{lm} R^2,$$
(3.7)

so then all the *R* dependence cancels out in the radiation zone, and we are left with

$$\tau_i^{\text{PP}} = \frac{1}{6\pi} \int (d\mathbf{r}) \frac{d\omega}{2\pi} i\omega^3 \epsilon_{ijk} \Im \chi_{kj}(\mathbf{r};\omega) \coth \frac{\beta'\omega}{2}.$$
 (3.8)

The only part of the anti-Hermitian part of the susceptibility that survives in this integral is the real, antisymmetric part of the susceptibility:

$$\operatorname{Im}\Im\chi_{kj} = -\frac{1}{2}[\operatorname{Re}\chi_{kj} - \operatorname{Re}\chi_{jk}],\tag{3.9}$$

so, introducing the mean polarizability

$$\alpha_{kj}(\omega) = \int (d\mathbf{r}) \chi_{kj}(\mathbf{r}; \omega),$$
 (3.10)

we have

$$\tau_{i} = \epsilon_{ijk} \int \frac{d\omega}{2\pi} \frac{\omega^{3}}{6\pi} \operatorname{Re} \alpha_{jk}(\omega) \left(\coth \frac{\beta \omega}{2} - \coth \frac{\beta' \omega}{2} \right),$$
(3.11)

where we have included the corresponding EE-fluctuation terms, (2,0) and (0,2). The only additional feature those terms bring in is that, because of the imaginary part of the Green's dyadic that arises because of the FDT, we must recognize the asymptotic replacement:

$$e^{i\omega R}\sin\omega R \to \frac{i}{2}, \quad e^{-i\omega R}\cos\omega R \to \frac{1}{2}.$$
 (3.12)

Thus, we have rederived, but by a rather more elaborate calculation, the nonreciprocal result (2.6).

B. Second-order torque

When we go to second order, we have to proceed more delicately. In particular, the **HH** part of the stress tensor contributes equally to the radiated angular momentum, so let us start with that. Classically, the corresponding contribution to the torque is

$$\tau_i^H = -\int d\Omega \int \frac{d\omega}{2\pi} \frac{d\nu}{2\pi} R^2 \,\hat{\mathbf{R}} \cdot \mathbf{H}(\mathbf{r}; \omega) \, (\mathbf{H}(\mathbf{r}; \nu) \times \mathbf{R})_i \, e^{-i(\omega + \nu)t}, \quad \mathbf{H}(\mathbf{r}; \omega) = \frac{1}{i\omega} \nabla \times \mathbf{E}(\mathbf{r}; \omega). \tag{3.13}$$

We expand E, as before, in successive powers of the generalized susceptibilities. The (3,1) and (1,3) expansions refer to PP fluctuations, which we will detail for the case of isotropic susceptibility. The (3,1) contribution is

$$\tau_{i}^{H(3,1)} = -\oint d\Omega R^{2} \int (d\mathbf{r})(d\mathbf{r}')(d\mathbf{r}'') \frac{d\omega}{2\pi} \frac{d\nu}{2\pi} \hat{R}_{l} \frac{\epsilon_{lmn}}{i\omega} \nabla_{m} \Gamma_{nk}(\mathbf{R} - \mathbf{r}; \omega) \chi(\mathbf{r}; \omega) \Gamma_{kp}(\mathbf{r} - \mathbf{r}'; \omega) P_{p}(\mathbf{r}'; \omega)
\times \frac{\epsilon_{iqr}}{i\nu} \epsilon_{qst} \nabla_{s} \Gamma_{tu}(\mathbf{R} - \mathbf{r}''; \nu) P_{u}(\mathbf{r}''; \nu) R_{r} e^{-i(\omega + \nu)t}
= -\oint d\Omega R^{2} \int (d\mathbf{r})(d\mathbf{r}') \frac{d\omega}{2\pi} \hat{R}_{l} \frac{\epsilon_{lmn}}{i\omega} \nabla_{m} \Gamma_{nk}(\mathbf{R} - \mathbf{r}; \omega) \chi(\mathbf{r}; \omega) \Gamma_{kp}(\mathbf{r} - \mathbf{r}'; \omega) \operatorname{Im} \chi(\mathbf{r}'; \omega)
\times \frac{\epsilon_{iqr}}{-i\omega} \epsilon_{qst} \nabla_{s} \Gamma_{tp}(\mathbf{R} - \mathbf{r}'; -\omega) R_{r} \coth \frac{\beta'\omega}{2}, \tag{3.14}$$

where, in the second line, we have used the FDT. Now we must do a better approximation for the Green's dyadic, in principle, keeping first-order corrections in both the exponent and the power terms:

$$\Gamma_{nk}(\mathbf{R} - \mathbf{r}; \omega) \sim \frac{1 - \mathbf{r} \cdot \nabla}{4\pi} \left[\frac{\omega^2}{R} (\mathbf{1} - \hat{\mathbf{R}}\hat{\mathbf{R}}) + \frac{i\omega}{R^2} (\mathbf{1} - 3\hat{\mathbf{R}}\hat{\mathbf{R}}) \right]_{nk} e^{i\omega(R - \hat{\mathbf{R}} \cdot \mathbf{r})}.$$
(3.15)

⁶Now (n, m) refers to n iterations of the first factor and m iterations of the second.

In this case, however, neither the $\mathbf{r} \cdot \nabla$ nor the subleading $i\omega/R^2$ terms need be retained, but this is not true for the **EE** terms. Now the effect of the first gradient in Eq. (3.14) is confined to the exponential:

$$\frac{1}{i\omega}\nabla_{m}e^{i\omega(R-\hat{\mathbf{R}}\cdot\mathbf{r})} = \left(\hat{R}_{m} - \frac{\mathbf{r}}{R}\cdot(\mathbf{1} - \hat{\mathbf{R}}\hat{\mathbf{R}})_{m}\right)e^{i\omega(R-\hat{\mathbf{R}}\cdot\mathbf{r})}.$$
(3.16)

The terms involving R_m vanish by virtue of the Levi-Civita symbol. Thus, Eq. (3.16) already provides the necessary \mathbf{r} factor. For the third Green's dyadic, we merely keep the leading term:

$$\frac{\nabla_s}{-i\omega}e^{-i\omega(R-\mathbf{r}'\cdot\hat{\mathbf{R}})} \sim \hat{R}_s e^{-i\omega(R-\mathbf{r}'\cdot\hat{\mathbf{R}})}.$$
 (3.17)

Putting this together, we have

$$\tau_{i}^{H(3,1)} = \oint d\Omega \int (d\mathbf{r})(d\mathbf{r}') \frac{d\omega}{2\pi} \frac{\omega^{4}}{(4\pi)^{2}} \chi(\mathbf{r};\omega)$$

$$\times \operatorname{Im} \chi(\mathbf{r}';\omega) \operatorname{coth} \frac{\beta'\omega}{2} e^{i\omega \hat{\mathbf{R}} \cdot (\mathbf{r}' - \mathbf{r})} \epsilon_{lmn} \hat{R}_{l} r_{m}$$

$$\times \Gamma_{np}(\mathbf{r} - \mathbf{r}';\omega) (\delta_{ip} - \hat{R}_{i} \hat{R}_{p}). \tag{3.18}$$

Now let us again abbreviate $\mathbf{v} = \omega(\mathbf{r}' - \mathbf{r})$ and work out the averages,

$$\oint d\Omega \hat{R}_l e^{i\hat{\mathbf{R}} \cdot \mathbf{v}} = 4\pi i \gamma v_l,$$

$$\oint d\Omega \hat{R}_l \hat{R}_m \hat{R}_n e^{i\hat{\mathbf{R}} \cdot \mathbf{v}} = 4\pi i [\alpha v_l v_m v_n + \beta (v_l \delta_{mn} + v_m \delta_{nl} + v_n \delta_{lm})].$$
(3.19a)

The coefficients γ , β , and α are immediately obtained by differentiating

$$\oint d\Omega \, e^{i\lambda \hat{\mathbf{R}} \cdot \mathbf{v}} = \frac{4\pi}{v\lambda} \sin v\lambda, \tag{3.20}$$

once or three times, with respect to $i\lambda$. The relevant results are

$$\gamma = \frac{\sin v}{v^3} - \frac{\cos v}{v^2},\tag{3.21a}$$

$$\alpha = -15 \frac{\sin v}{v^5} + 15 \frac{\cos v}{v^4} + 6 \frac{\sin v}{v^3} - \frac{\cos v}{v^2}, \quad (3.21b)$$

$$\beta = 3\frac{\sin v}{v^5} - 3\frac{\cos v}{v^4} - \frac{\sin v}{v^3}.$$
 (3.21c)

As we will immediately see, the α term does not contribute. Finally, we can write the internal Green's dyadic as

$$\mathbf{\Gamma}(\mathbf{r} - \mathbf{r}'; \omega) = f(v)\hat{\mathbf{v}}\hat{\mathbf{v}} + g(v)\mathbf{1}, \tag{3.22}$$

with

$$f(v) = \frac{\omega^3}{4\pi v^3} (3 - 3iv - v^2)e^{iv},$$
 (3.23a)

$$g(v) = -\frac{\omega^3}{4\pi v^3} (1 - iv - v^2)e^{iv}.$$
 (3.23b)

Then, it is readily seen that this contribution to the torque is

$$\boldsymbol{\tau}^{H(3,1)} = \frac{1}{4\pi} \int (d\mathbf{r})(d\mathbf{r}') \frac{d\omega}{2\pi} \omega^5 \operatorname{Re}\chi(\mathbf{r};\omega)$$

$$\times \operatorname{Im}\chi(\mathbf{r}';\omega)(\mathbf{r} \times \mathbf{r}') \operatorname{Im}[\gamma g(v) + \beta f(v)] \coth \frac{\beta'\omega}{2}$$

$$= \frac{1}{(4\pi)^2} \int (d\mathbf{r})(d\mathbf{r}') \frac{d\omega}{2\pi} \omega^8 X(\mathbf{r},\mathbf{r}';\omega)(\mathbf{r} \times \mathbf{r}')$$

$$\times \frac{1}{4v^8} \phi(v) \coth \frac{\beta'\omega}{2}, \qquad (3.24)$$

where ϕ is the function defined in Eq. (2.18). This result is exactly 1/4 of the PP part of Eq. (2.19). Indeed, following precisely the same procedure detailed here, the H (1, 3), the E (1, 3), and the E (3, 1) contributions are all the same, giving a PP contribution to the torque exactly as found in Eq. (2.19). We leave it to the reader to verify that the EE fluctuations give the corresponding structure, with the replacement of the thermal factor $\coth \beta'\omega/2 \rightarrow -\coth \beta\omega/2$. Note that only the (2, 2) **EE** and **HH** contributions are nonzero. As in Sec. II, again we conclude that inhomogeneity is required for both torque and force, in second order.

IV. EXAMPLE 1: DUAL ALLEN WRENCH

We now wish to study an example of an object that can exhibit a torque but not a net force, so one could study the rotational effect of a small object under a microscope. To preclude a force on an inhomogeneous object, we can require that it be reflection invariant about a central point. In order that it have a torque, the body must then be chiral, meaning that it cannot be transformed into any mirror reflection by a translation or a rotation. A simple example of such an object is shown in Fig. 1. The object is an L-shaped figure reflected in the top of the L, which we might call a dual Allen wrench, constructed of thin⁸ wires, with a shaft A of half length a lying in the y direction, and asymmetric end tags B of length b oriented along the x direction. The only significant domain of integration is along the wires, which have small cross-sectional areas S_A and S_B , respectively. The geometric integral (2.21b) then points perpendicularly to the plane of the body (the z axis), and is simple if we regard the cross-sectional radius as negligible in size:

$$\mathbf{J}_{AB}(\omega) = 2S_A S_B \omega^4 \hat{J}_{AB}(\omega) \hat{\mathbf{z}},$$

$$\hat{J}_{AB}(\omega) = \omega^4 \int_{-a}^a dy \int_0^b dx \, xy \frac{\phi(v)}{v^8},$$

$$v = \omega \sqrt{x^2 + (a+y)^2}.$$
(4.1)

Due to the positivity condition noted at the end of Sec. II, it is evident that $J_{AB} > 0$, which means the torque (2.21a) is

 $^{^{7}}$ To resolve any notational confusion, recall that *E* or **EE** refers to a term in the stress tensor (3.2b), while EE refers to the FDT contribution (2.3b).

⁸Thin, because we want the thickness to be less than the skin depth for the weak susceptibility approximation to be valid.

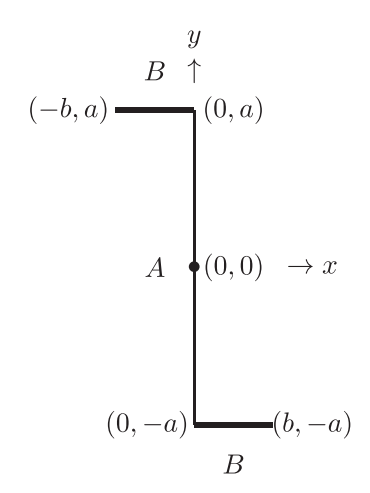


FIG. 1. A reflected L-shaped body ("dual Allen wrench") composed of a thin wire A (cross-sectional area S_A) of length 2a connected at the ends to perpendicular equal-length wires B (cross-sectional area S_B) each of length b. Shown also are the Cartesian coordinates of the center and the end points of the wire segments. The two components have respective susceptibilities χ_A , χ_B . This object is evidently invariant under reflection in the origin (0,0), but is chiral, so it will experience a quantum vacuum torque about an axis perpendicular to the plane of the figure, but not a force.

negative, clockwise in the sense of Fig. 1, if the susceptibility product $X_{AB} > 0$ and T' > T. Because the function ϕ involves significant cancellations, it is not very practical to integrate (4.1) numerically. Instead, it is convenient to adopt polar coordinates:

$$\tilde{x} \equiv \omega x = \rho \cos \theta, \quad \tilde{y} \equiv \omega (y + a) = \rho \sin \theta,$$
 (4.2)

where the integration is restricted to the interior of the rectangle with sides $2\tilde{a} \equiv 2\omega a$ and $\tilde{b} \equiv \omega b$. The result of straightforward integration on θ is

$$\hat{J}_{AB}(\omega) = -\tilde{a} \int_{0}^{2\tilde{a}} d\rho \frac{\phi(\rho)}{\rho^{6}} + \int_{\tilde{b}}^{\sqrt{\tilde{b}^{2} + 4\tilde{a}^{2}}} d\rho \frac{\phi(\rho)}{\rho^{6}} \left[\tilde{a} \sqrt{1 - \frac{\tilde{b}^{2}}{\rho^{2}}} + \frac{\tilde{b}^{2}}{2\rho} \right] + \frac{1}{2} \left[\int_{0}^{\tilde{b}} - \int_{2\tilde{a}}^{\sqrt{\tilde{b}^{2} + 4\tilde{a}^{2}}} d\rho \frac{\phi(\rho)}{\rho^{5}}, \quad (4.3)$$

which holds whatever are the relative magnitudes of 2a and b. Most of the ρ integrals can also be carried out in closed form. This function is always positive and, apart from the prefactor, is plotted in Fig. 2.

If both \tilde{a} and \tilde{b} are large, the asymptotic value of \hat{J}_{AB} arises only from the first integral in Eq. (4.3), and is

$$\hat{J}_{AB} \sim \frac{11}{30}\pi \tilde{a}, \quad \tilde{a} \gg 1.$$
 (4.4)

How large an object does this correspond to? If T and T' are both around room temperature, the transition between a "small" and a "large" object occurs when $a,b\approx 1/T\approx 10\,\mu\text{m}$, which uses the conversion factor $\hbar c=2\,\times$

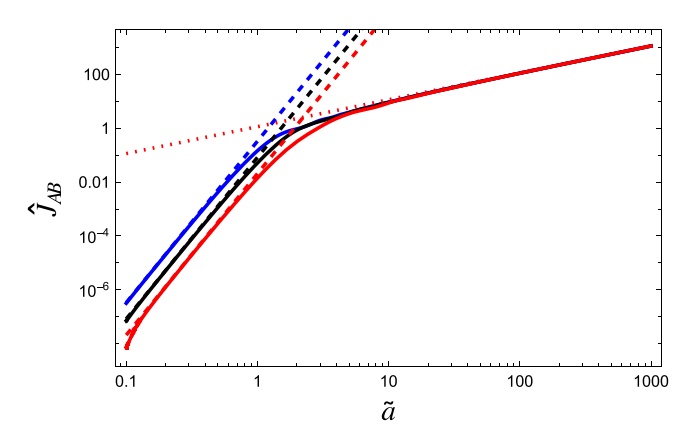


FIG. 2. The geometrical factor \hat{J}_{AB} in Eq. (4.3) plotted in terms of the scaled half length \tilde{a} of the central axis of the object in Fig. 1. The solid curves show the cases $\tilde{a} = \tilde{b}$ (central, black), $\tilde{b} = 2\tilde{a}$ (upper, blue), and $\tilde{a} = 2\tilde{b}$ (lower, red). Also displayed are the asymptotic values for large \tilde{a} and \tilde{b} (dotted red line), which show no dependence on the aspect ratio r = b/a, and the behaviors for both \tilde{a} and \tilde{b} small, which do show significant dependence on r, by the dashed lines. The transition between the two asymptotic regimes occurs over a relatively small region around $\tilde{a} = 2$.

 10^{-5} eV cm. Perhaps unexpectedly, this limit is independent of the aspect ratio r=a/b, and is depicted in Fig. 2. The physical explanation of the large \tilde{a} behavior of \hat{J}_{AB} is rather simple. The local interactions are dominated by the regions near the corners of the object. So, holding a fixed and increasing the lengths of the tags, b, rather quickly saturates the integral, and the torque becomes independent of b. This is true even for smaller values of \tilde{a} , as shown in Fig. 3. The local forces at the corners also saturate as \tilde{a} increases, but the lever arm grows linearly with a, so the integral and torque do as well.

Therefore, for a large object of the type shown in Fig. 1, with the shaft A being made of gold, described by a Drude susceptibility (nominal values taken from Ref. [51])

$$\chi_A = -\frac{\omega_p^2}{\omega^2 + i\omega \nu}, \quad \omega_p = 9 \,\text{eV}, \quad \nu = 0.035 \,\text{eV}, \quad (4.5)$$

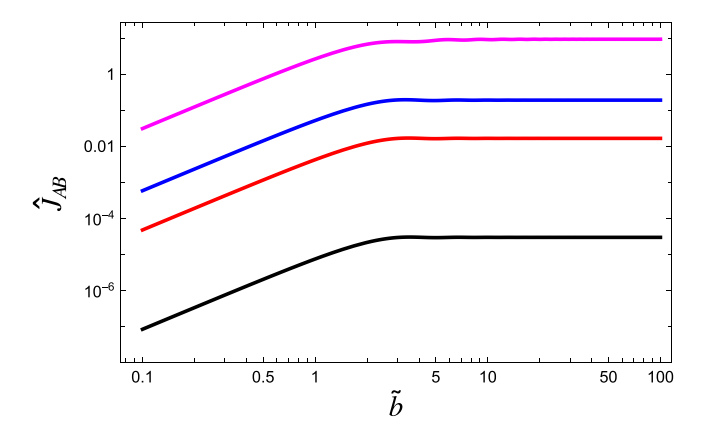


FIG. 3. The dependence the geometric factor \hat{J}_{AB} on \tilde{b} for fixed \tilde{a} . The four curves are for \tilde{a} equal to 0.1, 0.5, 1, and 10, from bottom to top. The curves are entirely similar, simply increasing with \tilde{a} .

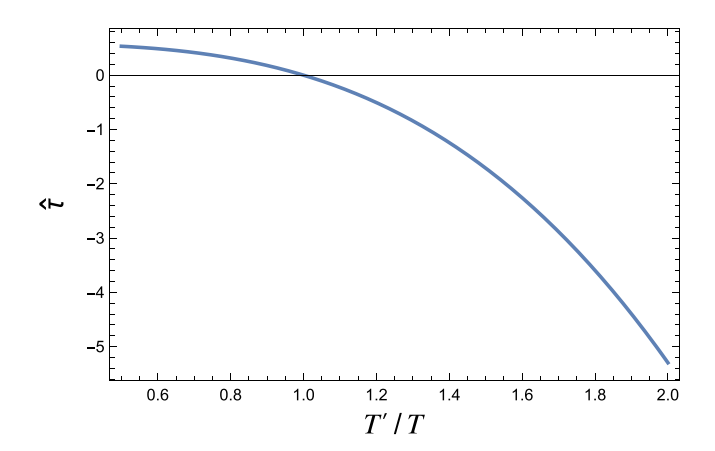


FIG. 4. The integral $\hat{\tau}$ in Eq. (4.6) as a function of the temperature of the body, T', relative to that of a vacuum environment at T = 300 K, for parameters as given in the text.

and the tags B made of a dispersionless material, we have for the torque

$$\tau = \frac{11}{60\pi^2} S_A S_B a v^4 \omega_p^2 \chi_B \int_0^\infty dx \frac{x^4}{x^2 + 1} \times \left(\frac{1}{e^{\beta \nu x} - 1} - \frac{1}{e^{\beta' \nu x} - 1} \right). \tag{4.6}$$

For a wire of circular radius 50 nm, which is approximately the skin depth of gold [48], with a=1 cm, the prefactor, τ_0 , evaluates to 7×10^{-22} N m. The integral, denoted $\hat{\tau}$, is shown in Fig. 4. Such a torque might well be observable.

On the other hand, as is most easily seen from the Cartesian form of J_{AB} (4.1) using the small v behavior of ϕ seen in Eq. (2.22a), the behavior of the geometric factor for a small object is

$$\hat{J}_{AB} = \frac{56}{675} \tilde{a}^6 r^2, \quad r = b/a, \quad \tilde{a}, \ \tilde{b} \ll 1.$$
 (4.7)

The contribution to J_{AB} from the leading term in $\phi(v)$ in the small argument limit (2.22a) vanishes by symmetry, so this result reflects the v^{10} term. This limit is also displayed in Fig. 2. It agrees well with the exact evaluation for $\tilde{a} < 1$. In this regime we can also readily calculate the torque for the same model for the constitution of the chiral object:

$$\tau = \frac{28}{675\pi^3} \chi_B v^9 \omega_p^2 S_A S_B a^4 b^2 [f_9(t) - f_9(t')],$$

$$f_n(t) \equiv \int_0^\infty dx \frac{x^n}{x^2 + 1} \frac{1}{e^{x/t} - 1},$$
(4.8)

where the dimensionless torque is

$$\hat{\tau} = f_9(t) - f_9(t'), \quad t = \frac{T}{v}, \quad t' = \frac{T'}{v},$$
 (4.9a)

and explicitly

$$f_9(t) = \Gamma(8)\zeta(8)t^8 - \Gamma(6)\zeta(6)t^6 + \Gamma(4)\zeta(4)t^4 - \Gamma(2)\zeta(2)t^2 - \frac{1}{2} \left[\psi\left(\frac{1}{2\pi t}\right) + \ln 2\pi t + \pi t\right].$$
 (4.9b)

The temperature dependence of $\hat{\tau}$ is shown in Fig. 5.

As noted below Eq. (4.1), if the body is hotter than the environment, the torque is always negative, that is, clockwise;

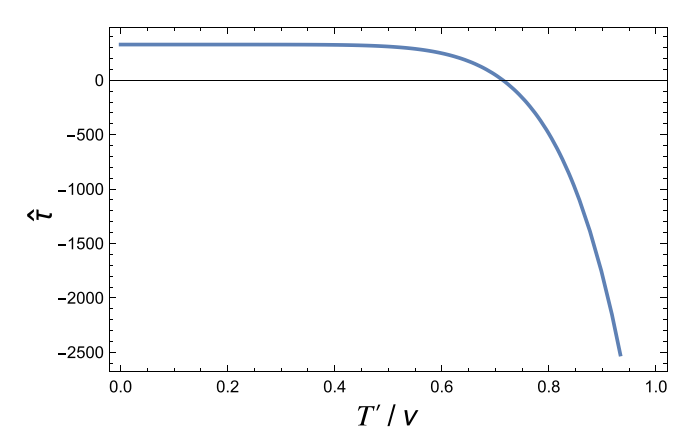


FIG. 5. The torque on a small Allen wrench, $\hat{\tau}$, apart from the prefactor, for the environmental vacuum temperature of 300 K for the configuration considered above, with $\nu = 0.035$ eV. For a = b = 1 µm, and a common cross-sectional radius of the wires being 40 nm (dictated by the skin depth [48]), the prefactor in Eq. (4.8) evaluates to 3.4×10^{-16} nN µm, which is rather large.

this is because the underlying local forces are always toward the metal side, that is, in the +x direction at the top, and the -x direction at the bottom, using the coordinate system of Fig. 1.

Terminal angular velocity

A chiral object, once set in rotation by a quantum vacuum torque, will feel quantum frictional forces opposing the motion. More important, however, will be the cooling of the object, if it is hotter than the environment, or heating otherwise. Both of these effects will cause the object to reach a final terminal angular velocity.

The initial angular acceleration α about the z axis is given by

$$I\alpha = \tau,$$
 (4.10)

where, for the object pictured in Fig. 1, the moment of inertia is

$$I = m_A \frac{1}{3}a^2 + m_B \left(a^2 + \frac{1}{3}b^2\right)$$

= $\rho_A S_A \frac{2}{3}a^3 + \rho_B S_B 2b \left(a^2 + \frac{1}{3}b^2\right)$, (4.11)

with m_A and m_B being the total masses of the A and B portions of the object. Let us suppose, in the perturbative spirit in which we are proceeding, that the cooling comes only from the metal, since in our simplified model only the A part of the object has an imaginary part to its susceptibility. According to Ref. [43] the power radiated by a Drude metal is

$$P(T, T') = \frac{1}{\pi^2} 2aS_A \nu^3 \omega_p^2 p(T, T'),$$

$$p(T, T') = f_3(T/\nu) - f_3(T'/\nu).$$
 (4.12)

⁹Realistically, this is at odds with the fact that the emissivity of a dielectric is much greater than that of a metal. This point is clarified in Appendix B.

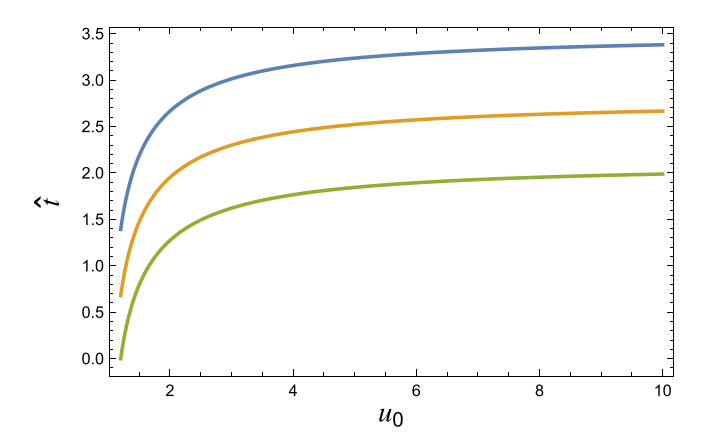


FIG. 6. Time taken (scaled by the prefactor t_0) for the object shown in Fig. 1 to cool from an initial temperature $T_0' = u_0 T$, to a final temperature $T_1' = u_1 T$. Here T is taken to be room temperature, 300 K, $\nu = 0.035$ eV, and the three curves are for different final temperature ratios $u_1 = 1.05$, 1.10, and 1.20, shown from top to bottom. The curves are similar, and plateau for large T_0' .

Since this is the rate of energy loss by the particle, the time t for the body to cool from temperature T_0' to T_1' , $T_0' > T_1' > T$, is [43]

$$t = \int_{T_0'}^{T_1'} dT' \frac{C_V(T')}{P(T, T')} = t_0 \hat{t}.$$
 (4.13)

If we suppose the specific heat $C_V(T) \approx 3N$, N being the number of atoms in A, which is the result of the Debye model for temperature well above the Debye temperature, $\Theta \approx 170 \text{ K}$ for gold (atomic mass $m_{\rm Au}$),

$$t_0 = \frac{3\pi^2 \rho_{\text{Au}} T}{m_{\text{Au}} \omega_n^2 \nu^3} \approx 30 \,\mu\text{s},$$
 (4.14a)

putting in parameters appropriate for gold. The remaining dimensionless integral is

$$\hat{t}(u_0, u_1; T) = \int_{u_0}^{u_1} du \frac{1}{p(u; T)}, \quad u = \frac{T'}{T}.$$
 (4.14b)

The latter is readily integrated and is shown in Fig. 6. It actually takes an infinitely long time to cool the body to equilibrium with the environment, but one can get arbitrarily close to the ambient temperature in a finite time.

Because of this cooling, the quantum torque on the body gradually decreases, until it finally reaches a terminal angular velocity given by integrating Eq. (4.10):

$$\omega_T = \frac{1}{I} \int_0^\infty dt \, \tau(T'(t), T) = \frac{t_0 \tau_0}{I} \hat{\omega}_T,$$

$$\hat{\omega}_T = \int_{u_0}^1 du \frac{\hat{\tau}(u; T)}{p(u; T)},$$
(4.15)

where we have changed variable from \hat{t} to u according to Eq. (4.14b). Using Eq. (4.6) for a large object, and ignoring the mass of the dielectric tags, we find the prefactor in ω_T to be roughly, for a wire of circular cross-sectional radius 50 nm and length 1 cm,

$$\frac{t_0 \tau_0}{I} \approx \frac{33}{40} \frac{S_B \nu T}{m_{\Delta \nu} a^2} \approx 5 \times 10^{-10} \,\mathrm{s}^{-1},$$
 (4.16)

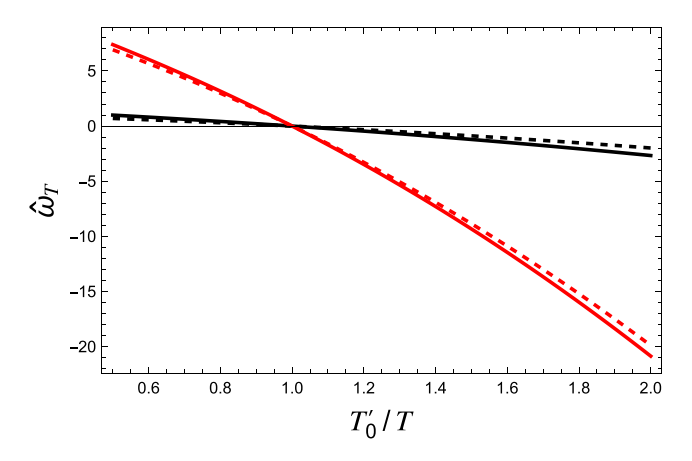


FIG. 7. The terminal angular velocity for the object shown in Fig. 1, apart from the prefactor, (4.16), as a function of the initial temperature of the body relative to the vacuum temperature. The latter is taken to be 300 K in the curves with lower slope (black) and 3000 K in the higher slope curves (red). In both cases, ν is taken to be 0.035 eV. The solid curves are the exact numerical integration, while the dashed lines are for the high-temperature approximation. The relative error is much smaller in the latter case.

which would seem to be undetectably small. The integral, $\hat{\omega}_T$, is shown in Fig. 7, and does not change this conclusion. Note that the rotation changes from clockwise to counterclockwise if the object is colder than the environment, because it is then absorbing radiant energy from the environment.

A more observable effect will arise for a small object, where the torque is given by Eq. (4.8). The initial acceleration when \tilde{a} , $\tilde{b} \ll 1$ is, for the representative case that $S_A = S_B$, a = b.

$$\alpha_0 = \frac{\tau}{I} = \frac{14}{225\pi^3} \chi_B v^9 \omega_p^2 S_A a^3 \frac{1}{\rho_A + 4\rho_B} [f_9(T/\nu) - f_9(T'/\nu)]$$

$$\equiv \frac{\tau_0}{I} \hat{\tau}, \qquad (4.17)$$

where f_9 is the function defined in Eq. (4.9b). The prefactor τ_0 for our nominal values for gold, and $a=b=1~\mu m$, is about $5\times 10^{-3}~{\rm s}^{-2}$. The cooling time prefactor t_0 does not depend on the dimensions of the A wire, so is still $30~\mu s$, as given in Eq. (4.14a). The terminal angular velocity, given by Eq. (4.15), where the prefactor is now $t_0\tau_0/I\approx 2\times 10^{-7}~{\rm s}^{-1}$, is nearly three orders of magnitude bigger than the corresponding prefactor for the large-argument limit (4.16). The remaining integral is

$$\hat{\omega}_T = \int_{u_0}^1 du \frac{f_9(t) - f_9(t')}{f_3(t) - f_3(t')}, \quad t = \frac{T}{\nu}, \quad t' = \frac{T'}{\nu}, \quad (4.18)$$

where the functions $f_{2k+1}(t)$, with k a positive integer, are given in Eq. (4.8), which are explicitly

$$f_{2k+1}(t) = \Gamma(2k)\zeta(2k)t^{2k} - \Gamma(2k-2)\zeta(2k-2)t^{2k-2} + \cdots$$

$$+ (-1)^{k+1}\Gamma(2)\zeta(2)t^{2}$$

$$+ (-1)^{k+1}\frac{1}{2}\left[\psi\left(\frac{1}{2\pi t}\right) + \ln 2\pi t + \pi t\right]. \quad (4.19)$$

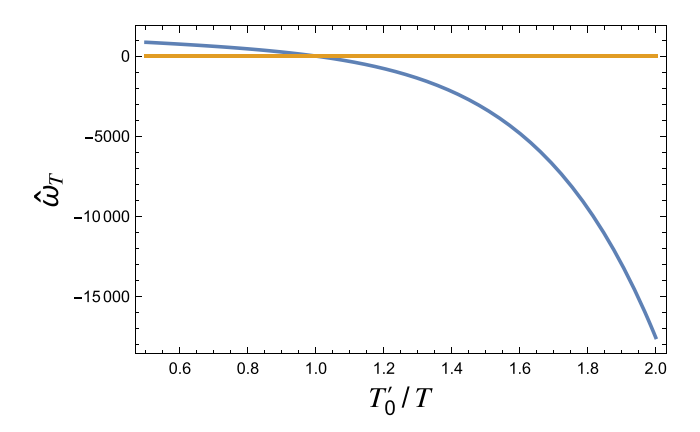


FIG. 8. The dimensionless integral $\hat{\omega}_T$, Eq. (4.18), in the terminal angular velocity for a small Allen wrench object as a function of the initial temperature T_0' of the object, relative to the temperature of the vacuum background $T=300~{\rm K}, \nu=0.035~{\rm eV}$. This integral is typically much larger than the corresponding $\hat{\omega}_T$ shown in Fig. 7 for a large Allen wrench.

The resulting numerical integral for $\hat{\omega}_T$ is shown in Fig. 8. So, for the object initially at twice the ambient temperature, the terminal angular velocity would be $3 \times 10^{-3} \text{ s}^{-1}$, which should be readily observable.

V. EXAMPLE 2: DUAL FLAG

We now consider a two-dimensional model, in which the tags of the first example are replaced by thin plates, which we will call flags, with sides b and a, and thickness L_B , as shown in Fig. 9.

The torque on this object is still given by Eq. (2.21). Evidently, only the z component of the geometric integral is nonzero, which, rather immediately, reduces to the threefold

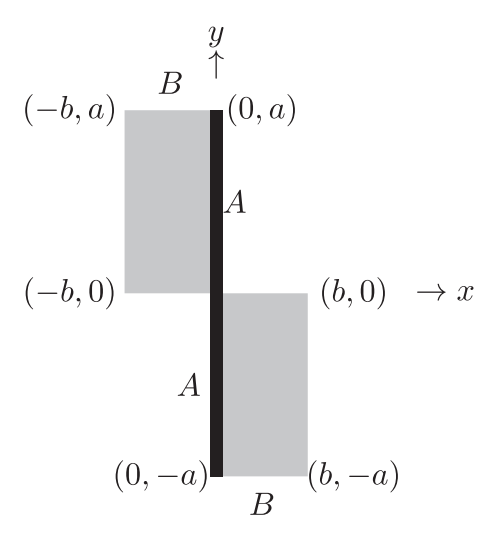


FIG. 9. A two-dimensional chiral object, consisting of a central metallic wire A of length 2a and cross-sectional area S_A , from which dielectric flags, of height a, width b, and thickness L_B , extend to the left for the upper flag, and to the right for the lower flag. The whole assembly is reflection invariant about the central point, denoted by (0,0), so there is no net self-propulsive force on the object.

integral, because both flags contribute equally:

$$J_{AB}(\omega) = 2S_A L_B \int_{-a}^{a} dy \int_{-b}^{0} dx' \int_{0}^{a} dy'$$

$$\times \frac{yx'}{[x^2 + (y - y')^2]^4} \phi \left[\omega \sqrt{x^2 + (y - y')^2}\right]. \quad (5.1)$$

We adopt dimensionless variables.

$$\tilde{x} = \omega x, \quad \tilde{y} = \omega y, \quad \tilde{y}'' = \omega (y' - y), \quad (5.2)$$

so the y integral is trivial, and we are left with

$$J_{AB}(\omega) = -\omega^3 S_A L_B \int_0^{\tilde{b}} d\tilde{x}' \left[2 \int_0^{\tilde{a}} d\tilde{y}''(\tilde{a}^2 - \tilde{y}''^2) + \int_0^{2\tilde{a}} d\tilde{y}''(\tilde{y}''^2 - 2\tilde{a}\tilde{y}'') \right] \frac{\tilde{x}'}{v^8} \phi(v), \quad v = \sqrt{\tilde{x}'^2 + \tilde{y}''^2}, \tag{5.3}$$

where $\tilde{a} = \omega a$, $\tilde{b} = \omega b$. Now we adopt polar coordinates,

$$\tilde{y}'' = v \sin \theta, \quad \tilde{x}' = v \cos \theta,$$
 (5.4)

where, with due attention to the limits of integration, the integral over θ can be readily carried out. In terms of the radial integrals

$$\Phi(\alpha, \beta, n) \equiv \int_{\alpha}^{\beta} dv \frac{\phi(v)}{v^n},\tag{5.5a}$$

$$\Psi(\alpha, \beta, n) \equiv \int_{\alpha}^{\beta} dv \frac{\phi(v)}{v^n} \sqrt{1 - \frac{\alpha^2}{v^2}},$$
 (5.5b)

we find

$$J_{AB}(\omega) = -\omega^{3} S_{A} L_{B} \left\{ -\frac{1}{3} \Phi(0, \tilde{a}, 4) + \frac{1}{3} \Phi(\tilde{a}, 2\tilde{a}, 4) - \tilde{a} \Phi(0, \tilde{b}, 5) + \tilde{a} \Phi\left(2\tilde{a}, \sqrt{4\tilde{a}^{2} + \tilde{b}^{2}}, 5\right) + 2\tilde{a}^{2} \Phi(0, \tilde{a}, 6) \right.$$

$$\left. - \tilde{a} \tilde{b}^{2} \Phi\left(\tilde{b}, \sqrt{4\tilde{a}^{2} + \tilde{b}^{2}}, 7\right) + \frac{4}{3} \tilde{a}^{3} \Phi\left(\tilde{a}, \sqrt{\tilde{a}^{2} + \tilde{b}^{2}}, 7\right) - \frac{4}{3} \tilde{a}^{3} \Phi\left(2\tilde{a}, \sqrt{4\tilde{a}^{2} + \tilde{b}^{2}}, 7\right) + \frac{2}{3} \Psi\left(\tilde{b}, \sqrt{\tilde{a}^{2} + \tilde{b}^{2}}, 4\right) \right.$$

$$\left. - \frac{1}{3} \Psi\left(\tilde{b}, \sqrt{4\tilde{a}^{2} + \tilde{b}^{2}}, 4\right) - \frac{2}{3} \left(3\tilde{a}^{2} + \tilde{b}^{2}\right) \Psi\left(\tilde{b}, \sqrt{\tilde{a}^{2} + \tilde{b}^{2}}, 6\right) + \frac{1}{3} \tilde{b}^{2} \Psi\left(\tilde{b}, \sqrt{4\tilde{a}^{2} + \tilde{b}^{2}}, 6\right) \right\}$$

$$(5.6)$$

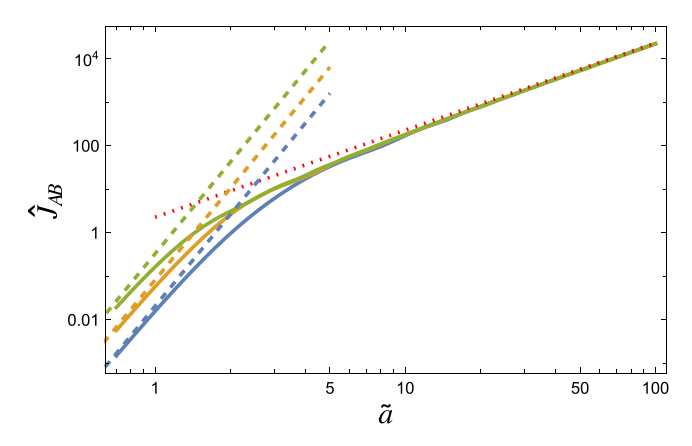


FIG. 10. Reduced geometric integrals \hat{J}_{AB} as a function of $\tilde{a} = a\omega$ are shown for b = a/2, b = a, and b = 2a from bottom to top. The dotted red line shows the behavior for large \tilde{a} , while the dashed lines show the small \tilde{a} behavior. The transition between these asymptotes occurs for $\tilde{a} \approx 2$, that is, around $a = 20 \, \mu m$ for frequencies corresponding to room temperature. As with the Allen wrench, the dependence on \tilde{b} disappears for large \tilde{a} .

The Φ integrals can all be given in closed form in terms of sine-integral functions, while the Ψ integrals seem to require numerics. In Fig. 10 we show the geometric integral $\hat{J}_{AB}(\tilde{a}, \tilde{b})$, defined by $J_{AB}(\omega) = \omega^3 S_A L_B \hat{J}_{AB}(\tilde{a}, \tilde{b})$.

For large \tilde{a} , the leading term comes only from $\Phi(0, a, 6)$ in Eq. (5.6), as in the Allen wrench model, and is, as follows from Eq. (2.22b),

$$\hat{J}_{AB}(\tilde{a}, \tilde{b}) \sim \frac{11\pi}{15} \tilde{a}^2, \quad \tilde{a} \gg 1,$$
 (5.7a)

independent of \tilde{b} , while the small argument expansion (2.22a) gives

$$\hat{J}_{AB}(\tilde{a}, \tilde{b}) \sim \frac{56}{675} \tilde{a}^5 \tilde{b}^2, \quad \tilde{a}, \, \tilde{b} \ll 1$$
 (5.7b)

These are also compared to the exact results in Fig. 10. The results are quite comparable to the geometric integral for the Allen wrench. In fact, comparing the full geometric integrals in the small- and large-frequency limits,

$$\frac{J_{AB}^{\text{DF}}}{J_{AB}^{\text{AW}}} \sim \frac{aL_B}{S_B} \begin{cases} 1, & \omega a \gg 1, \\ \frac{1}{2}, & \omega a \ll 1. \end{cases}$$
 (5.8)

This indicates that the geometric integrals in the two models differ only by roughly the geometric ratio of the size of the object divided by its thickness. Of course, the moment of inertia of the larger object, the dual flag, is somewhat bigger:

$$I^{\text{DF}} = \frac{1}{3} [m_A a^2 + m_B (a^2 + b^2)]$$

= $\frac{2}{3} a [\rho_A S_A a^2 + \rho_B L_B b (a^2 + b^2)],$ (5.9)

where m_i is the mass of the *i*th component of the object. However, typically the mass of the metal wire is much larger than that of the flags, so this results in only a small correction. The torque for a large dual flag ($a \gg 10 \, \mu \text{m}$ for room temperature) is thus different from that of the Allen wrench (4.6) by precisely the above factor given in Eq. (5.8):

$$\tau = \frac{11}{60\pi^2} a^2 S_A L_B \chi_B \omega_p^2 \nu^4 [f_4(T/\nu) - f_4(T'/\nu)]$$
 (5.10)

The cooling of the object, due primarily to the metal wire, is unchanged. For a = b = 1 cm and $L_B = 50$ nm, the enhancement factor is

$$\frac{aL_B}{S_B} \sim \frac{a}{L_B} \approx 10^5,\tag{5.11}$$

resulting in a terminal velocity of $\omega_T \approx 10^{-4} \, \mathrm{s}^{-1}$. For a small object, so that $\tilde{a} \sim \tilde{b} \ll 10$ µm, the enhancement factor is about 10, which increases the terminal velocity to about $\omega_T \approx 3 \times 10^{-2} \, \mathrm{s}^{-1}$ for $T = 300 \, \mathrm{K}$ and $T' = 600 \, \mathrm{K}$. These enhancements increase the likelihood of observing these terminal angular velocities.

VI. CONCLUSIONS

In this paper we have extended the considerations of Ref. [48] to the torque on an inhomogeneous chiral body in vacuum, out of thermal equilibrium with the blackbody radiation. We do this by carrying out a perturbative expansion in powers of the electric susceptibility of the body. In first order, a torque can only arise if the susceptibility is nonreciprocal, which usually entails an external field of some kind. To get a true vacuum effect on a body made of reciprocal material in second order requires only one additional requirement: the body must be inhomogeneous. A body made of uniform material cannot experience a vacuum torque, at least through second order. ¹⁰

We develop a general formalism for the torque, both by directly calculating the torque, and looking at the angular momentum flux carried away from the body at infinity. The general approach also allows for nonisotropic susceptibilities, and arbitrary inhomogeneity. We restrict attention, for simplicity, to the case when all parts of the inhomogeneous body are at a common temperature.

We then consider some simple examples of bodies composed of two contiguous parts, each of which has a uniform isotropic electric susceptibility. We present explicit results when one part is a dispersionless dielectric and the other part is a Drude metal. We choose configurations for which there is no net force, but only a torque. The sense of the torque is given by that of the local forces between the two parts, which are dominated by the immediate region of the interface. If the body is hotter than the vacuum, these forces are always directed toward the metal side, due to the high reflectivity of the latter. Once the body is set rotating by the quantum vacuum torque, it will quickly reach a terminal angular velocity due to thermalization, unless a mechanism is provided to sustain the thermal imbalance. However, it seems likely that configurations can be found where such a terminal angular velocity could be observed in the laboratory. 11

¹⁰Ongoing investigations indicate that forces and torques do, in fact, appear in third order.

¹¹We speculate that such forces and torques might occur with living organisms, which indeed possess mechanisms to keep themselves out of thermal equilibrium.

ACKNOWLEDGMENTS

This work was supported in part by NSF Grant No. 2008417. We thank Steve Fulling, Xin Guo, and Prachi Parashar for collaborative assistance. This paper reflects solely the authors' personal opinions and does not represent the opinions of the authors' employers, present and past, in any way.

APPENDIX A: SUSCEPTIBILITY ORDERS IN E AND P EXPANSIONS

This Appendix shows how to obtain the terms to each order in the generalized susceptibilities in E and P expansions, in a compact form that easily keeps track of orders and factors. The focus is on the structure of terms and expressions. The exposition is symbolic: no boldface, no integrals, delta func-

tions implied as factors of unity, and transpositions include coordinate variables as well as indices.

We begin by splitting the full E and P fields into their corresponding free (or fluctuating) (f) and induced (i) parts:

$$E = E^f + E^i \tag{A1a}$$

and

$$P = P^f + P^i, (A1b)$$

where

$$E^i = \Gamma P \tag{A2a}$$

and

$$P^i = \chi E \tag{A2b}$$

Note that only the free (fluctuating) parts are used in the relevant FDT. Then

$$E = E^f + \Gamma(P^f + \chi E) \Rightarrow E = (1 - \Gamma \chi)^{-1} (E^f + \Gamma P^f) = \sum_{n=0}^{\infty} (\Gamma \chi)^n (E^f + \Gamma P^f) = \sum_{m=0}^{\infty} E^{(m)}$$
(A3a)

and

$$P = P^f + \chi(E^f + \Gamma P) \Rightarrow P = (1 - \chi \Gamma)^{-1} (P^f + \chi E^f) = \sum_{n=0}^{\infty} (\chi \Gamma)^n (P^f + \chi E^f) = \sum_{m=0}^{\infty} P^{(m)},$$
 (A3b)

where m denotes the number of generalized susceptibility factors in these expansions. It immediately follows that

$$E^{(m)} = \begin{cases} (\Gamma \chi)^{\frac{m}{2}} E^f, & \text{if } m \text{ is even,} \\ (\Gamma \chi)^{\frac{m-1}{2}} \Gamma P^f, & \text{if } m \text{ is odd,} \end{cases}$$
(A4a)

and

$$P^{(m)} = \begin{cases} (\chi \Gamma)^{\frac{m}{2}} P^f, & \text{if } m \text{ is even,} \\ (\chi \Gamma)^{\frac{m-1}{2}} \chi E^f, & \text{if } m \text{ is odd.} \end{cases}$$
(A4b)

Products such as $\langle PE \rangle$ may be similarly decomposed, yielding

$$\langle PE \rangle = \sum_{m=0}^{\infty} \sum_{n=0}^{\infty} \langle P^{(m)} E^{(n)} \rangle$$

$$= \sum_{m \text{ even } n \text{ odd}}^{\infty} \sum_{n \text{ odd}}^{\infty} \langle P^{(m)} E^{(n)} \rangle + \sum_{m \text{ odd } n \text{ even}}^{\infty} \langle P^{(m)} E^{(n)} \rangle, \quad (A5a)$$

which becomes

$$\langle PE \rangle = \sum_{m \text{ even } n \text{ odd}}^{\infty} \operatorname{tr} \left\{ (\Gamma \chi)^{\frac{n-1}{2}} \Gamma P^{c} (\Gamma^{T} \chi^{T})^{\frac{m}{2}} \right\}$$

$$+ \sum_{m \text{ odd } n \text{ even}}^{\infty} \operatorname{tr} \left\{ (\chi \Gamma)^{\frac{m-1}{2}} \chi E^{c} (\chi^{T} \Gamma^{T})^{\frac{n}{2}} \right\}, \qquad (A5b)$$

where $P^c \equiv \langle P^f P^f \rangle$ and $E^c \equiv \langle E^f E^f \rangle$ are the free (fluctuating) field correlation functions (symmetrization understood), to be evaluated using the relevant FDT. Of course, this last expression may be written in different forms.

Where ∇ operators are involved in expressions, these should be inserted at appropriate places in expansions such as the above.

APPENDIX B: DUALITY BETWEEN DIELECTRIC-METAL AND BLACKBODY-METAL COMPOSITES

In the text we point out that the local interactions between the disparate portions of the composite body are such that the effective forces between a dispersionless dielectric and a Drude metal are in the direction of the metal. In Ref. [48] we saw in an example that this was also true if the dielectric were replaced by an ideal blackbody. This is a general feature: Up to a factor, the second-order susceptibility factor is the same for the two situations. Suppose χ_A is given by Eq. (4.5), while χ_B is a real constant. Then, the susceptibility factor is

$$X_{AB}(\omega) = \chi_B \frac{\omega_p^2 \nu}{\omega(\omega^2 + \nu^2)}$$
 (B1)

On the other hand, an ideal blackbody has a surface susceptibility of [48]

$$\tilde{\chi}_B(\omega) = \frac{i}{4} \frac{1}{\omega + i\epsilon}, \quad \epsilon \to +0,$$
 (B2)

so using that for χ_B we have

$$X_{AB} = \frac{1}{4\omega t} \frac{\omega_p^2}{\omega^2 + v^2},\tag{B3}$$

where t is the thickness of the blackbody surface. These two susceptibility factors, (B1) and (B3), are the same function of ω , and hence yield the same torques, up to a constant

factor. Now the blackbody is a perfect emitter, if T' > T, while the Drude metal is a good reflector, so it seems clear that more radiation is emitted on the blackbody side of the

composite object, resulting in a force toward the metal side. This argument seems less ambiguous than that based on the dielectric-metal composite.

- [1] E. V. Teodorovich, Contribution of macroscopic van der Waals interactions to frictional force, Proc. R. Soc. A **362**, 71 (1978).
- [2] L. S. Levitov, Van der Waals friction, Europhys. Lett. 8, 499 (1989).
- [3] J. B. Pendry, Shearing the vacuum—Quantum friction, J. Phys.: Condens. Matter 9, 10301 (1997).
- [4] A. I. Volokitin and B. N. J. Persson, Theory of friction: The contribution from a fluctuating electromagnetic field, J. Phys.: Condens. Matter 11, 345 (1999).
- [5] G. V. Dedkov and A. A. Kyasov, The relativistic theory of fluctuation electromagnetic interactions of moving neutral particles with a flat surface, Phys. Solid State 45, 1815 (2003).
- [6] P. C. W. Davies, Quantum vacuum friction, J. Opt. B 7, S40 (2005).
- [7] G. Barton, On van der Waals friction. II: Between atom and half-space, New J. Phys. 12, 113045 (2010).
- [8] R. Zhao, A. Manjavacas, F. J. G. de Abajo, and J. B. Pendry, Rotational quantum friction, Phys. Rev. Lett. 109, 123604 (2012).
- [9] M. G. Silveirinha, Theory of quantum friction, New J. Phys. 16, 063011 (2014).
- [10] G. Pieplow and C. Henkel, Cherenkov friction on a neutral particle moving parallel to a dielectric, J. Phys.: Condens. Matter 27, 214001 (2015).
- [11] F. Intravaia, V. E. Mkrtchian, S. Y. Buhmann, S. Scheel, D. A. R. Dalvit, and C. Henkel, Friction forces on atoms after acceleration, J. Phys.: Condens. Matter 27, 214020 (2015).
- [12] J. S. Høye, I. Brevik, and K. A. Milton, The reality of Casimir friction, Symmetry **8**, 29 (2016).
- [13] G. V. Dedkov and A. A. Kyasov, Nonlocal friction forces in the particle-plate and plate-plate configurations: Nonretarded approximation, Surf. Sci. 700, 121681 (2020).
- [14] M. B. Farías, F. C. Lombardo, A. Soba, P. L. Villar, and R. Decca, Towards detecting traces of non-contact quantum friction in the corrections of the accumulated geometric phase, npj Quantum Inf. 6, 25 (2020).
- [15] M. Oelschläger, Fluctuation-induced phenomena in nanophotonic systems, Ph.D. thesis, Institut für Physik, Humboldt Universität zu Berlin, 2020.
- [16] G. V. Dedkov, Nonequilibrium Casimir-Lifshitz friction force and anomalous radiation heating of a small particle, Appl. Phys. Lett. 121, 231603 (2022).
- [17] T.-B. Wang, Y. Zhou, H.-Q. Mu, K. Shehzad, D.-J. Zhang, W.-X. Liu, T.-B. Yu, and Q.-H. Liao, Enhancement of lateral Casimir force on a rotating body near a hyperbolic material, Nanotechnology 33, 245001 (2022).
- [18] I. Brevik, B. Shapiro, and M. G. Silveirinha, Fluctuational electrodynamics in and out of equilibrium, Int. J. Mod. Phys. A 37, 2241012 (2022).
- [19] Z. Xu, P. Ju, K. Shen, Y. Jin, Z. Jacob, and T. Li, Observation on non-contact Casimir friction, arXiv:2403.06051.
- [20] A. Einstein and L. Hopf, Statistische untersuchung der bewegung eines resonators in einem strahlungsfeld, Ann. Phys. (Leipzig) **338**, 1105 (1910).

- [21] V. Mkrtchian, V. A. Parsegian, R. Podgornik, and W. M. Saslow, Universal thermal radiation drag on neutral objects, Phys. Rev. Lett. 91, 220801 (2003).
- [22] G. V. Dedkov and A. A. Kyasov, Tangential force and heating rate of a neutral relativistic particle mediated by equilibrium background radiation, Nucl. Instrum. Methods Phys. Res., Sect. B 268, 599 (2010).
- [23] G. Łach, M. DeKieviet, and U. D. Jentschura, Einstein-Hopf drag, Doppler shift of thermal radiation and blackbody drag: Three perspectives on quantum friction, Cent. Eur. J. Phys. 10, 763 (2012).
- [24] G. Pieplow and C. Henkel, Fully covariant radiation force on a polarizable particle, New J. Phys. 15, 023027 (2013).
- [25] A. I. Volokitin, Friction force at the motion of a small relativistic neutral particle with respect to blackbody radiation, JETP Lett. 101, 427 (2015).
- [26] A. I. Volokitin and B. N. J. Persson, *Electromagnetic Fluctuations at the Nanoscale* (Springer-Verlag, Berlin, 2017).
- [27] X. Guo, K. A. Milton, G. Kennedy, W. P. McNulty, N. Pourtolami, and Y. Li, Energetics of quantum vacuum friction: Field fluctuations, Phys. Rev. D 104, 116006 (2021).
- [28] X. Guo, K. A. Milton, G. Kennedy, W. P. McNulty, N. Pourtolami, and Y. Li, Energetics of quantum vacuum friction. II: Dipole fluctuations and field fluctuations, Phys. Rev. D 106, 016008 (2022).
- [29] D. Reiche, F. Intravaia, J.-T. Hsiang, K. Busch, and B.-L. Hu, Nonequilibrium thermodynamics of quantum friction, Phys. Rev. A 102, 050203(R) (2020).
- [30] C. Khandekar, S. Buddhiraju, P. R. Wilkinson, J. K. Gimzewski, A. W. Rodriguez, C. Chase, and S. Fan, Nonequilibrium lateral force and torque by thermally excited nonreciprocal surface electromagnetic waves, Phys. Rev. B 104, 245433 (2021).
- [31] D. Gelbwaser-Klimovsky, N. Graham, M. Kardar, and M. Krüger, Near field propulsion forces from nonreciprocal media, Phys. Rev. Lett. 126, 170401 (2021).
- [32] M. Krüger, T. Emig, and M. Kardar, Nonequilibrium electromagnetic fluctuations: Heat transfer and interactions, Phys. Rev. Lett. **106**, 210404 (2011).
- [33] A. Ott, P. Ben-Abdallah, and S.-A. Biehs, Circular heat and momentum flux radiated by magneto-optical nanoparticles, Phys. Rev. B 97, 205414 (2018).
- [34] M. F. Maghrebi, A. V. Gorshkov, and J. D. Sau, Fluctuation-induced torque on a topological insulator out of thermal equilibrium, Phys. Rev. Lett. **123**, 055901 (2019).
- [35] D. Pan, H. Xu, and F. J. García de Abajo, Magnetically activated rotational vacuum friction, Phys. Rev. A 99, 062509 (2019).
- [36] C. Khandekar and Z. Jacob, Thermal spin photonics in the near-field of nonreciprocal media, New J. Phys. **21**, 103030 (2019).
- [37] H. C. Fogedby and A. Imparato, Autonomous quantum rotator, Europhys. Lett. 122, 10006 (2018).
- [38] C. Guo and S. Fan, Theoretical constraints on reciprocal and non-reciprocal many-body radiative heat transfer, Phys. Rev. B 102, 085401 (2020).

- [39] Y. Guo and S. Fan, A single gyrotropic particle as a heat engine, ACS Photon. **8**, 1623 (2021).
- [40] B. Strekha, S. Molesky, P. Chao, M. Krüger, and A. Rodriguez, Trace expressions and associated limits for non-equilibrium Casimir torque, Phys. Rev. A 106, 042222 (2022).
- [41] L. Ge, Negative vacuum friction in terahertz gain systems, Phys. Rev. B **108**, 045406 (2023).
- [42] V. S. Asadchy, M. S. Mirmoosa, A. Diaz-Rubio, S. Fan, and S. A. Tretyakov, Tutorial on electromagnetic nonreciprocity and its origins, Proc. IEEE **108**, 1684 (2020).
- [43] K. A. Milton, X. Guo, G. Kennedy, N. Pourtolami, and D. M. DelCol, Vacuum torque, propulsive forces, and anomalous tangential forces: Effects of nonreciprocal media out of thermal equilibrium, Phys. Rev. A 108, 022809 (2023).
- [44] G. Kennedy, Quantum torque on a non-reciprocal body out of thermal equilibriium and induced by a magnetic field of arbitrary strength, Eur. Phys. J. Spec. Top. 232, 3197 (2023).
- [45] L. Zhu, Y. Guo, and S. Fan, Theory of many-body radiative heat transfer without the constraint of reciprocity, Phys. Rev. B 97, 094302 (2018).

- [46] B. Müller and M. Krüger, Anisotropic particles near surfaces: Propulsive force and friction, Phys. Rev. A 93, 032511 (2016).
- [47] M. T. H. Reid, O. D. Miller, A. G. Polimeridis, A. W. Rodriguez, E. M. Tomlinson, and S. G. Johnson, Photon torpedoes and Rytov pinwheels: Integral-equation modeling of non-equilibrium fluctuation-induced forces and torques on nanoparticles, arXiv:1708.01985.
- [48] K. A. Milton, N. Pourtolami, and G. Kennedy, Quantum self-propulsion of an inhomogeneous object out of thermal equilibrium, Phys. Rev. A 110, 042814 (2024).
- [49] J. R. Deop-Ruano, F. J. García de Abajo, and A. Manjavacas, Thermal radiation forces on planar structures with asymmetric optical response, Nanophotonics 13, 4569 (2024).
- [50] K. Milton and J. Schwinger, Classical Electrodynamics, 2nd ed. (CRC, Boca Raton, FL, 2024).
- [51] A. Lambrecht and S. Reynaud, Casimir force between metallic mirrors, Eur. Phys. J. D 8, 309 (2000).